

Magnetoplasma effects in a quasi-three-dimensional electron gas

K. Karrai, H. D. Drew, and M. W. Lee

*Joint Program for Advanced Electronic Materials, Department of Physics and Astronomy,
University of Maryland, College Park, Maryland 20742
and Laboratory for Physical Sciences, College Park, Maryland 20742*

M. Shayegan

*Department of Electrical Engineering, Princeton University, Princeton, New Jersey 08544
(Received 26 September 1988)*

Far-infrared magnetotransmission measurements on a quasi-three-dimensional modulation-doped semiconductor structure are reported in the frequency region of the bulk plasmon. When a magnetic field is applied tilted with respect to the film plane, two branches appear in the excitation spectrum resulting from the coupling between cyclotron resonance and the plasma oscillations perpendicular to the film plane. The experiment demonstrates the connection between the depolarization-shifted intersubband transitions and the bulk plasma resonance.

Magnetically induced collective phenomena in electron-gas systems have stimulated considerable theoretical attention;^{1,2} however, little experimental work has been reported on the three-dimensional (3D) electron gas in semiconductors. A variety of collective effects such as charge-density waves, spin-density waves, and Wigner crystallization have been predicted^{1,2} for a 3D electron gas and they should be enhanced by application of an intense magnetic field at very low temperatures. The observed behavior of a 3D *uniformly* doped semiconductor in a strong magnetic field, however, is dominated by the electron-impurity interaction, leaving the above-mentioned collective phenomena yet unobserved.¹⁻³ Recently a way to grow a conducting layer which is nearly free of impurities and which is sufficiently thick that some three-dimensional effects may occur was suggested by Gossard and Halperin.¹ Such structures have now been grown by using a graded $\text{Al}_x\text{Ga}_{1-x}\text{As}$ quantum well and modulation-doped $\text{Al}_y\text{Ga}_{1-y}\text{As}$ barriers ($y > x$).^{4,5} In these structures a nearly uniform density of electrons $n \approx 2 \times 10^{16}/\text{cm}^3$ was obtained over a range $\cong 1000 \text{ \AA}$ thick with donors removed several hundred angstroms from either side of the quantum well.

In this Rapid Communication we report far-infrared magnetotransmission on these structures undertaken in order to investigate possible quasi-three-dimensional (Q3D) properties of the confined electron gas. One characteristic 3D property is the bulk plasma resonance excited by the normal component of the radiation field at frequency $\omega_p = (ne^2/m^*\epsilon_s)^{1/2}$, where n is the electron density, m^* the electron effective mass, and ϵ_s the static dielectric constant of the medium.⁶ In bulk, degenerately doped semiconductors, mode coupling between the bulk plasmon, and the cyclotron motion is observed in experiments in which the magnetic field is tilted with respect to the surface normal.^{7,8} In similar experiments performed on 2D electron gas systems the observed resonances are interpreted in terms of coupling between the cyclotron motion and the plasma-shifted intersubband reso-

nances.⁹⁻¹² In this Rapid Communication we report the first observation of plasma-cyclotron coupled motion in a Q3D electron gas. The experiment demonstrates the connection between the 3D plasma resonance and the 2D plasma shifted intersubband resonance.

In order to achieve a Q3D electron gas with a nearly uniform electron density, it is necessary to provide a confining potential, $V_0(z)$ tailored to cancel the Hartree potential of the free electrons. The appropriate potential, in the classical limit, is the negative of the Poisson potential of a homogeneous electron gas of the desired concentration n_0 . Therefore, $V_0(z) = \frac{1}{2}(n_0e^2/\epsilon_s)z^2$, where ϵ_s is the static dielectric constant, and z is the distance in the growth direction. For a low density of electrons of mass m^* , this confinement potential gives rise to a harmonic oscillator spectrum with frequency $\omega_0 = (n_0e^2/\epsilon_sm^*)^{1/2}$. This harmonic spectrum is valid for electron areal density $n_s \ll n_0a$ where $a = (\hbar/m^*\omega_0)^{1/2}$ is the amplitude of the zero-point motion. For $n_s \gg n_0a$ the system behaves as a classical free-electron metal of thickness $t = n_s/n_0$ and the Hartree potential nearly cancels $V_0(z)$. The corresponding eigenstates are square well states in a well of width t . The experimentally realizable situation is the intermediate case and so the Schrödinger and Poisson equations must be solved self-consistently for the energy levels, wave functions, and total potential.

The samples used in this study consist of 2000- \AA -wide $\text{Al}_x\text{Ga}_{1-x}\text{As}$ sandwiched between two thick barriers of δ -doped $\text{Al}_{0.27}\text{Ga}_{0.73}\text{As}$ grown by molecular-beam epitaxy.⁴ The concentration of aluminum, x , was varied quadratically to provide the parabolic confining potential. Taking the conduction-band offset ΔE_c for GaAs/ $\text{Al}_x\text{Ga}_{1-x}\text{As}$ to be¹³ $\Delta E_c = 750x$ in units of meV and a design 3D density $n_0 = 2.1 \times 10^{16}/\text{cm}^3$, x was varied quadratically from 0 in the center of the well to $x = 0.19$ at the edges. Transport measurements on these samples⁴ showed 2D quantization in the slab at high magnetic fields applied in the z direction as manifested by the quantum Hall effect. From the transport measurements⁴ on the

sample reported on here it was concluded that there are $n_s = 2.5 \times 10^{11}/\text{cm}^2$ electrons in the well occupying four electric subbands at zero magnetic field. The mobility of this sample was in excess of $100\,000 \text{ cm}^2/\text{Vs}$. In this realization of the parabolic well $n_s/n_0a \cong 10$ is not very large so that we do not expect strict 3D behavior. Self-consistent calculations connecting the Poisson equation to the effective-mass Hamiltonian have been carried out in the Hartree approximation (ignoring exchange-correlation effects) for the energy levels and eigenfunctions for these wells. The zero-field results are consistent with the observed four subband occupation. The wave function and the energy level of the ground state in the presence of a 5 T magnetic field applied perpendicular to the slab is shown in Fig. 1. At this field only one spin degenerate Landau subband is filled.¹⁴ These calculations include the effective-mass variation of the electrons across the well in a BenDaniel and Duke¹⁵ type of Hamiltonian. For our sample parameters the two first calculated bound-state energies were found to be $E_0 = 4.11 \text{ meV}$ and $E_1 = 4.45 \text{ meV}$ at 5 T (the zero of energy is the band edge at the center of the well).

Far-infrared (FIR) magneto-transmission measurements were performed on these samples in the Faraday geometry with unpolarized light. The FIR radiation from a Fourier-transform spectrometer transmitted through the sample was measured with a composite bolometer detector operating at 1.4 K and located outside the magnetic field. The sample substrate was wedged 4° in order to avoid line-shape distortion due to interference fringes, and was cooled slowly in the dark to liquid-helium temperature. The angle, θ , between the applied magnetic field and the growth axis was varied by mounting the sample on a brass wedge and the corresponding angle was checked with an accuracy of $\pm 1.5^\circ$ by use of a He-Ne laser reflection on the epitaxial layer. Experiments were carried out at three angles: $\theta = 0^\circ$, 13° , and 30° . Typical FIR spectra at 0° tilt angle are shown in Fig. 2. The observed features are consistent with cyclotron resonance (CR) at all fields. This in itself is noteworthy since bulk

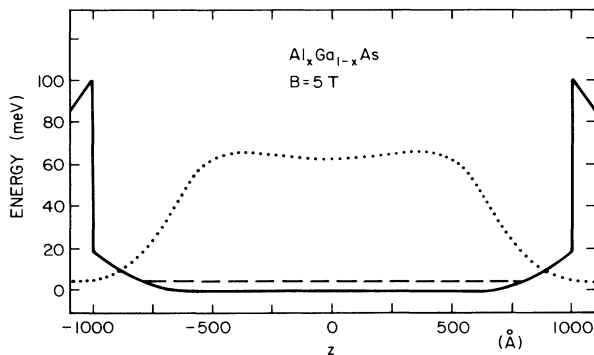


FIG. 1. Results of self-consistent calculations in the Hartree approximation for a parabolic quantum well. The solid curve is the self-consistent potential, the dotted curve is the ground-state energy, and the dashed curve is the corresponding wave function. The parameters were $n_0 = 2.1 \times 10^{16}/\text{cm}^3$ and $n_s = 2.4 \times 10^{11}/\text{cm}^2$. At 5 T only one Landau level is filled.

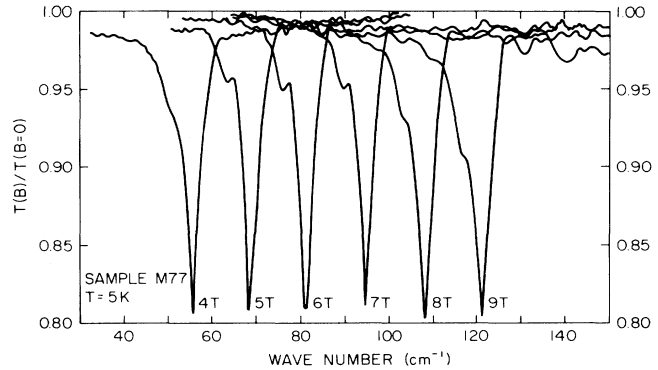


FIG. 2. Transmission spectra of the sample at various magnetic field for the case $\theta = 0^\circ$. Note the satellite peak on the low-frequency side of the resonance.

uniformly doped GaAs samples at densities $n \cong n_0$ undergo a magnetic-field-induced metal-insulator transition in this magnetic-field range and their FIR spectrum is dominated by inter-impurity-band optical transitions.¹⁶ The oscillator strength of the CR peaks in Fig. 2 is consistent with the electron density determined from transport data to within 10%. In the range $B > 2 \text{ T}$, the CR shows a striking asymmetry which appears to be a satellite absorption peak on the low-frequency side of the line. This satellite is well resolved only in the vicinity of 6 T. Tentatively, we understand this satellite peak in terms of the variation of the effective mass of the carriers across the graded quantum well,¹⁷ which leads to an effective cyclotron mass associated with each electric subband. Since the level widths correspond roughly to the separation between E_0 and E_1 , both levels are expected to be occupied (i.e., at any temperature). However, calculations based on the square well approximation to our well gives $m_{c0}^* = 0.068m_0$ for the ground subband and $m_{c1}^* = 0.0705m_0$ for the first excited state, which underestimates the splitting. We plan additional studies to clarify the nature of the CR line shape.

When the sample is tilted to 13° and 30° the cyclotron resonance splits into two branches as shown in Figs. 3 and 4. As the magnetic field increases the intensity of the low-frequency branch (ω^-) reduces, and its position first pinned to $\omega^- = \omega_c \cos\theta$ tends asymptotically to a frequency $\Omega_x \cos\theta$. As the intensity of the low-frequency resonance begins reducing and shifting from $\omega_c \cos\theta$, then a second branch (ω^+) at higher frequency appears initially pinned to Ω_x . As the field is further increased, ω^+ tends toward the CR frequency position determined from the 0° angle measurements. For both tilt angles the two branches “anticross” at 3.5 T and at $\Omega_x = 47.5 \pm 0.5 \text{ cm}^{-1}$. This position is determined by the condition that the oscillator strength of the two resonances are equal. As can be seen in Fig. 4 a gap opens up in the excitation spectrum between $\Omega_x \cos\theta$ and Ω_x .

The dispersion of the two branches, ω^\pm , follows the general relation for the resonant frequency of coupled harmonic oscillators having ω_c and $\Omega = \Omega_x$ as harmonic frequencies and whose polarization vectors are oriented

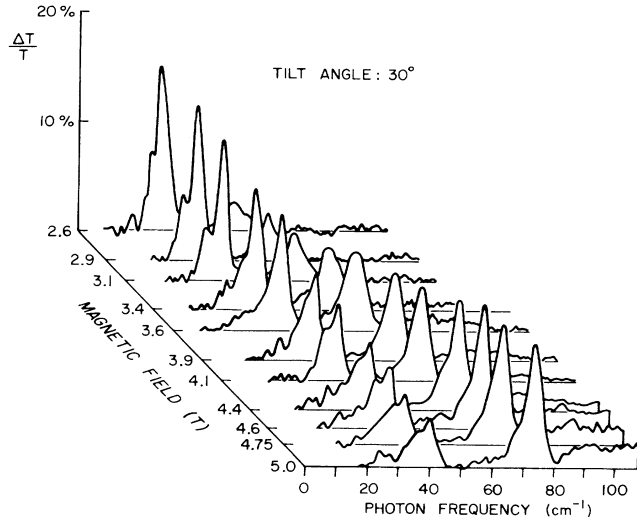


FIG. 3. Transmission spectra of the sample at various magnetic fields in 30° tilted angle showing the transfer of oscillator strength from the low- to the high-frequency branch as the magnetic field is increased. Note that the line-shape asymmetry remains in the tilted field resonances.

$\pi/2 - \theta$ apart. The ω^\pm are given by the roots of^{7,8,18}

$$1 = \frac{\Omega^2 \sin^2 \theta}{\omega^2 - \omega_c^2} - \frac{\Omega^2 \cos^2 \theta}{\omega^2}. \quad (1)$$

The value of Ω_x is close to the bare harmonic oscillator frequency ω_0 of the parabolic well given by Eq. (1). Taking $n_0 = 2.1 \times 10^{16}/\text{cm}^3$ and the observed $m^* = 0.068m_0$ and $\epsilon_s = 13$ we find $\omega_0 = 48 \text{ cm}^{-1}$. It is natural, therefore, to consider an interpretation of these data in terms of mode coupling between the cyclotron resonance and the

intersubband resonances of the bare parabolic well in tilted magnetic fields.¹⁸ At the measured electron density n_s , however, the condition $n_s \ll n_0 a$ is severely violated and the subband spacings of the self-consistent well potential are much smaller than Ω_x . Therefore, this interpretation can be rejected.

Ω_x is also close to the 3D plasma frequency ω_p . This coincidence is not accidental since $\omega_p \equiv \omega_0$ in the Hartree approximation. Therefore, it is interesting to consider these results within the classical 3D limit (i.e., ignoring the spatial quantization). In this case we have a 3D free-electron plasma spread uniformly in a slab whose effective thickness we parametrize as d . The parabolic potential provides a restoring force along the growth axis on the whole 3D electron gas and a plasmon of frequency ω_p can propagate along the growth direction. Once again the observed resonances are given^{7,8} by the roots of Eq. (1), where now Ω is the bulk plasma frequency ω_p . From $\Omega_x = \omega_p$ we deduce a 3D concentration $n = 2.2 \times 10^{16}/\text{cm}^3$. Comparing n and n_s we determine the effective thickness $d = 1100 \text{ \AA}$, which is comparable to the width of the uniform electron density region of the well as calculated in the Hartree approximation as can be seen in Fig. 1.

This success is surprising since it is more natural, in our experiments (where $n_s/n_0 a$ is not very large) to view the systems as 2D. This is especially clear from the observation of the quantum Hall effect⁴ and the occupation of only one electric and magnetic subband near and above the anticrossing field. Within the 2D context the interpretation of our results is expressed in terms of the mixed intersubband-cyclotron resonance modes.⁹⁻¹² As is well known these modes are shifted by the polarization fields induced by the component of the electric field normal to the plane.⁹ Ω_x is then the shifted optical intersubband resonance given by $\Omega_x^2 = \omega_{01}^2 + \tilde{\omega}_p^2$, where $\hbar\omega_{01} = E_1 - E_0$ is the intersubband spacing and $\tilde{\omega}_p$ is the depolarization and excitonlike contribution to the resonance frequency. It is

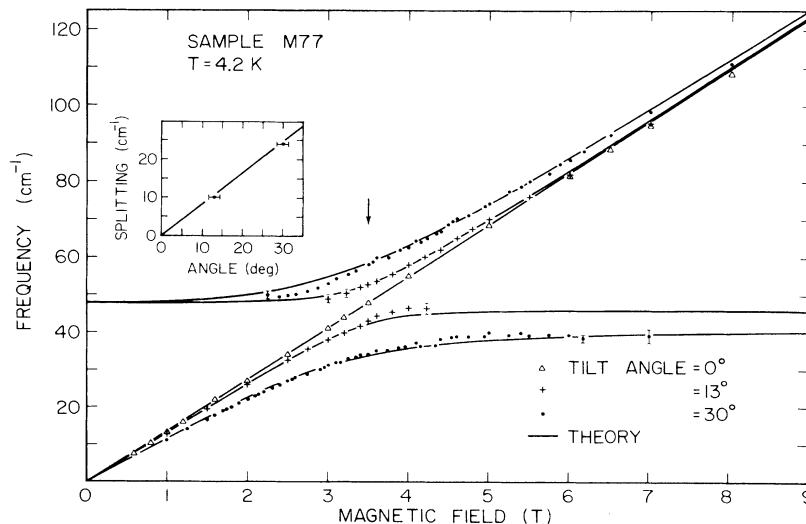


FIG. 4. Position of the minimum of transmission for 0° , 13° , and 30° angle compared to the normal modes of coupled harmonic oscillators given by the roots of Eq. (1). The anticrossing occurs at 3.5 T and $\Omega_x = 47.5 \text{ cm}^{-1}$.

important to note that in this wide quantum well the contribution of the intersubband energy is only of order 0.2% of the optical resonance frequency. The excitonlike shift, which arises from the exchange-correlation potential can be neglected for these very wide quantum wells.¹⁹

If we approximate our (self-consistent) quantum well as a square well of width d , the depolarization shift is calculated as $\tilde{\omega}_p^2 = \frac{5}{3} (n_s e^2 / d \epsilon_s m^*)$. Setting this equal to the experimental value for $\tilde{\omega}_p^2$ we find $d = 1900 \text{ \AA}$. The corresponding subband spacing in this square-well approximation is $\hbar \omega_{01} = E_1 - E_0 = 0.46 \text{ meV}$. In fact the positions of ω^\pm are not strictly given by the roots of Eq. (1) for the square well. Recent measurements have shown, however, that the coupled harmonic oscillators model for a square well is a very good approximation for the transition between the fundamental and first excited state.¹⁸

On the other hand, Eq. (1) rigorously applies for a parabolic well in the Hartree approximation.¹² Approximating our (self-consistent) quantum well as a parabolic well we calculate that $\tilde{\omega}_p^2 = (N_s e^2 / 1 \epsilon_s m^*) (2/\pi)^{1/2}$ for the transition from the fundamental to the first excited level, where $1 = (\hbar/m^* \omega_{01})^{1/2}$. Setting this estimate of $\tilde{\omega}_p$ equal to Ω_x we obtain $1 = 910 \text{ \AA}$ corresponding to $\hbar \omega_{01} = 0.14 \text{ meV}$. These two estimates of $\hbar \omega_{01}$ bracket the calculated value of 0.34 meV . We conclude from this analysis that the interpretation of Ω_x as the depolarization shifted $0 \rightarrow 1$ subband transition is plausibly demonstrated. To make a more quantitative analysis would require using the exact wave functions. However, uncertainties in the growth and material parameters make such an analysis unrewarding at this time.

We see with these several comparisons that reasonable agreement with the experiments is found both with the 2D analysis and with the classical 3D case. Due to the uncertainty in the true curvature of the well it is impossible to choose between the 2D and 3D interpretations or whether

they give identical results. The observed mode-coupling behavior involving the bulk plasmon is certainly expected in the limit as $n_s/n_0 a \rightarrow \infty$. What is surprising about the results reported here is that the behavior is already very 3D for $n_s/n_0 a \cong 10$ and only one occupied electric and magnetic subband over most of the interesting magnetic-field range of the experiment. Some insight into this behavior is obtained by noting that the $0 \rightarrow 1$ transition is much stronger than all the other intersubband transitions from the ground state. The oscillator strengths, f_n , associated with the bare conductivity are given¹² by $f_n = (2m^*/\hbar) \times \omega_n |\langle n | z | 0 \rangle|^2$, where $\omega_n = (E_n - E_0)/\hbar$. Within the square-well model we find $f_1 = 0.96$, $f_3 = 0.03$, $f_5 < 0.01$. Therefore, f_1 nearly exhausts the oscillator strength sum rule. This means that for frequencies $\omega \gg \omega_1$ the bare conductivity is very nearly of the classical 3D form $\sigma_{zz} \cong n_0 e^2 / m^* \omega$.

In conclusion, we have demonstrated that in our very wide quantum wells 3D character such as 3D plasma-cyclotron coupling tends to predominate while pure 2D aspects like intersubband optical transitions are mostly dominated by depolarization effects. Indeed, we are seeing the approach to the 3D limit of this 2D effect. These new type of structures containing a Q3D electron gas appear to be good candidates for studying magnetically induced collective phenomena predicted at very low temperatures in the 3D free-electron gas.

We thank Sankar Das Sarma, V. J. Goldman, and D. C. Tsui for useful discussions, D. Romero for technical assistance, and M. Santos and T. Sajoto for assistance in sample preparation. This work was supported by National Science Foundation Grant Nos. ECS-8553110, No. DMR-8705002, and No. DMR-8704670 and U.S. Office of Naval Research Grant No. N00014-86-K-0273.

¹B. I. Halperin, Jpn. J. Appl. Phys. **26**, Suppl. 26-3, 1913 (1987), and references therein.

²A. H. MacDonald and G. W. Bryant, Phys. Rev. Lett. **58**, 515 (1987).

³M. Shayegan, V. J. Goldman, and H. D. Drew, Phys. Rev. B **38**, 5585 (1988).

⁴M. Shayegan, T. Sajoto, M. Santos, and C. Silvestre, Appl. Phys. Lett. **53**, 791 (1988); M. Shayegan, M. Santos, T. Sajoto, K. Karräi, M-W. Lee, and H. D. Drew, in *Magnetic Fields in Semiconductor Physics, II*, edited by G. Landwehr (Spring-Verlag, Berlin, in press).

⁵M. Sundaram, A. C. Gossard, J. H. English, and R. M. Westervelt, Superlattices Microstruc. (to be published); E. G. Gwinn, P. F. Hopkins, A. J. Romberg, R. M. Westervelt, M. Sundaram, and A. C. Gossard, in *Magnetic Fields in Semiconductor Physics II*, edited by G. Landwehr (Spring-Verlag, Berlin, in press).

⁶S. Iwasa, Y. Samada, E. Burstein, and E. D. Palik, J. Phys. Soc. Jpn. Suppl. **21**, 742 (1966).

⁷I. B. Bernstein, Phys. Rev. **109**, 10 (1958).

⁸N. D. Mermin and E. Canel, Ann. Phys. (N.Y.) **26**, 247 (1964).

⁹See e.g. T. Ando, A. B. Fowler, and F. Stern, Rev. Mod. Phys. **54**, (1982).

¹⁰Z. Schlesinger, J. M. C. Hwang, and S. J. Allen, Phys. Rev. Lett. **50**, 2098 (1983).

¹¹M. Zaluzny, Solid State Commun. **55**, 747 (1985); **56**, 235 (1985).

¹²T. Ando, Z. Phys. B **26**, 263 (1977).

¹³See, e.g., R. C. Miller, A. C. Gossard, D. A. Kleinman, and O. Munteanu, Phys. Rev. B **29**, 3740 (1984); R. C. Miller, D. A. Kleinman, and A. C. Gossard, *ibid.* **29**, 7085 (1984).

¹⁴The spin splitting is very small and can be neglected in the analysis of these experiments.

¹⁵D. J. BenDaniel and C. B. Duke, Phys. Rev. **152**, 683 (1966); R. A. Morrow and K. R. Brownstein, Phys. Rev. B **30**, 678 (1984); H. C. Liu, Superlattices Microstruct. **3**, 413 (1987).

¹⁶M-W. Lee, D. Romero, H. D. Drew, M. Shayegan, and B. Elman, Solid State Commun. **66**, 23 (1988).

¹⁷M. Zachan, F. Koch, G. Weimann, and W. Schlapp, Phys. Rev. B **33**, 8564 (1986).

¹⁸R. Merlin, Solid State Commun. **64**, 99 (1987); R. Borroff, R. Merlin, R. L. Greene, and J. Comao, Superlattices Microstruct. **3**, 493 (1987).

¹⁹T. Ando, J. Phys. Soc. Jpn. **51**, 3893 (1982).